

New preparation method of $\text{La}_{n+1}\text{Ni}_n\text{O}_{3n+1-\delta}$ ($n=2, 3$)

Maria Deus Carvalho,^{*a} Fernanda Madalena A. Costa,^a Isabel da Silva Pereira,^a Alain Wattiaux,^{*b} Jean Marc Bassat,^b Jean Claude Grenier^b and Michel Pouchard^b

^aDepartamento de Química da Faculdade de Ciências da Universidade de Lisboa, Rua Ernesto de Vasconcelos, C1-5°, 1700 Lisboa, Portugal

^bInstitut de Chimie de la Matière Condensée de Bordeaux (ICMCB), CNRS, Avenue du Docteur Albert Schweitzer, 33 608 Pessac Cedex, France

Samples $\text{La}_{n+1}\text{Ni}_n\text{O}_{3n+1-\delta}$ ($n=2,3$) have been prepared by two different methods, which lead to different oxygen stoichiometry values. Materials obtained by the citrate route always show higher content of Ni^{3+} , which can be rationalized by the high reactivity and the original morphology of the precursors obtained by this method.

The ternary nickel oxides with the general formula $\text{La}_{n+1}\text{Ni}_n\text{O}_{3n+1}$, similar to the Ruddlesden–Popper series, show a multilayered crystal structure which can be described by the stacking along the c axis of n finite LaNiO_3 perovskite layers separated by LaO rocksalt-like layers.^{1,2}

Generally, it has been difficult to obtain pure phases of the $\text{La}_{n+1}\text{Ni}_n\text{O}_{3n+1}$ ($n=2,3$) series and often the referred phases exhibit intergrowth problems influencing their physical properties.^{3–5}

Recently, Zhang *et al.* prepared the $n=2$ member^{6,7} starting from an organic precursor and obtained a single-phase oxygen-deficient $\text{La}_3\text{Ni}_2\text{O}_{6.92}$. The stoichiometric phase with respect to the oxygen content was made by heating the as-prepared sample at high oxygen pressure. These authors had also prepared the stoichiometric $n=3$ member.⁸

Sreedhar *et al.*⁴ have observed that intergrowths occur only as isolated line defects for $n=2$ and $n=3$ members. These results have definitively shown the strong influence of the synthesis method on the stacking ordering as well as on the oxygen stoichiometry, which results in different Ni^{3+} contents and consequently in various physical and chemical properties (for the stoichiometric phases the mean oxidation state of nickel is 2.50 ($n=2$) and 2.67 ($n=3$), respectively).

It is well established that decomposition of precursors with small particle size and high surface area often allows one to prepare homogeneous pure phases inaccessible by conventional solid-state reactions.

The aim of this work was the preparation of the $n=2$ and $n=3$ members of this series, without intergrowth phenomena, using different methods.

A careful chemical analysis (lanthanum, nickel and oxygen contents) was also carried out in order to determine their exact formulation.

Experimental

The samples were prepared as follows.

1 Solid state route

Stoichiometric quantities of La_2O_3 (99.999%, dried at 1273 K prior to use) and NiO (99.99%) were mixed and heated in air at 1423 and 1353 K for the preparation of $\text{La}_3\text{Ni}_2\text{O}_{7-\delta}$ and $\text{La}_4\text{Ni}_3\text{O}_{10-\delta}$, respectively.

However, this conventional solid-state reaction always resulted in the formation of a phase mixture, even after prolonged heating as previously reported.⁶

2 Nitrate route

Stoichiometric amounts of NiO (99.99%) and La_2O_3 (99.999%, dried at 1273 K prior to use) were dissolved in nitric acid solution (*ca.* 1/3 HNO_3 , 2/3 H_2O).

This solution was fired to dryness and the resulting nitrates slowly decomposed on a hot plate. The dark gray products were ground and heated in air at 1173 K for 2 h. The black powder was annealed in air at 1423 and 1353 K in order to obtain $\text{La}_3\text{Ni}_2\text{O}_{7-\delta}$ and $\text{La}_4\text{Ni}_3\text{O}_{10-\delta}$, respectively. Several intermediate grindings were necessary and single-phase materials were obtained after heating for *ca.* 3 days for $\text{La}_3\text{Ni}_2\text{O}_{7-\delta}$ and 14 days for $\text{La}_4\text{Ni}_3\text{O}_{10-\delta}$.

3 Citrate route

Stoichiometric amounts of NiO (99.99%) and La_2O_3 (99.999%, dried at 1273 K prior to use) were dissolved in a slight excess of nitric acid solution followed by the addition of an equivalent molar proportion of citric acid with respect to NiO and La_2O_3 .

The solution was heated to dryness and the formation of a green gel was observed during this thermal treatment. Then, the product was gently heated on a sand bath which induces auto-combustion. Final thermal treatment was the same as for the nitrate route to allow a comparative study. A drastic decrease in reaction times could be observed by this route, especially for $\text{La}_4\text{Ni}_3\text{O}_{10-\delta}$ for which only 2 days were necessary to obtain a single phase.

The samples were characterized by powder X-ray diffraction using a Philips diffractometer with $\text{Cu-K}\alpha$ radiation. High-resolution transmission electron microscopy (HRTEM) was performed with a JEOL 2000FX electron microscope. SEM images were obtained with a JEOL JSM 35C and EDS analysis carried out with a Noran-Voyager apparatus. Nickel and lanthanum contents were measured by atomic absorption with a Unicam 929 AA spectrometer and using a Radiometer ion-selective electrode (ISE25F), respectively.

The oxygen non-stoichiometry content (δ) of all the samples was deduced from chemical analyses of trivalent nickel (τ) by a well known titration method [$\delta=(n-1-\tau)/2$] according to the formulation $\text{La}_{n+1}\text{Ni}_{(n-\tau)}^{2+}\text{Ni}_{\tau}^{3+}\text{O}_{3n+1-\delta}$.

Electrical resistivity measurements were carried out in the range 4.2–300 K on sintered pellets using a standard four-probe technique.⁹

Results and Discussion

1 Characterization of the precursors

SEM images of the precursors revealed significant differences in their morphology, depending on the preparation. SEM

images of the precursors obtained after auto-combustion (citrate route) and after decomposition on a hot plate (nitrate route) for $n=2$ and $n=3$ samples are shown in Fig. 1 and 2.

It is clear that, for both phases, the morphologies of the precursors obtained by the citrate and nitrate routes are completely different. The materials obtained by the citrate route are extremely thin, 'fly-wing' like particles without grains and agglomerates [Fig. 1, 2], in contrast to those prepared by the nitrate route. After heating for 2 h at 1173 K the SEM characteristics show similar differences for the two samples. However, the grain size of the powders obtained by the nitrate route is obviously bigger and agglomerates can be seen, which was not observed when using the citrate method. XRD studies of these precursors after annealing 2 h at 1173 K revealed that the citrate route leads to a mixture of different members of the series $\text{La}_{n+1}\text{Ni}_n\text{O}_{3n+1}$ for $n=2$ (nominal composition), but a single phase for $n=3$ [Fig. 3, 4]. Conversely, by the nitrate route, both precursors seem to be a mixture of different members of the series, La_2O_3 and NiO [Fig. 3, 4].

These results show the higher reactivity observed when preparing the samples by the citrate route; this is due to the original morphology of the precursors obtained by this rapid thermal procedure.¹⁰

2 $\text{La}_{n+1}\text{Ni}_n\text{O}_{3n+1}$ ($n=2,3$) compounds

The change in the X-ray pattern of each sample with time of reaction revealed that the kinetics in the citrate route is faster than in the nitrate route. After a heat treatment of 12 h at the annealing temperature ($T=1423$ K for $n=2$, $T=1353$ K for $n=3$), the X-ray data revealed single phases for the samples obtained with the citrate precursors, while by the nitrate route, they showed a mixture of different phases. This feature was observed for both prepared phases ($n=2$ and $n=3$).

The XRD patterns for the final materials prepared by both routes are identical as can be seen in Fig. 5 and 6, with only

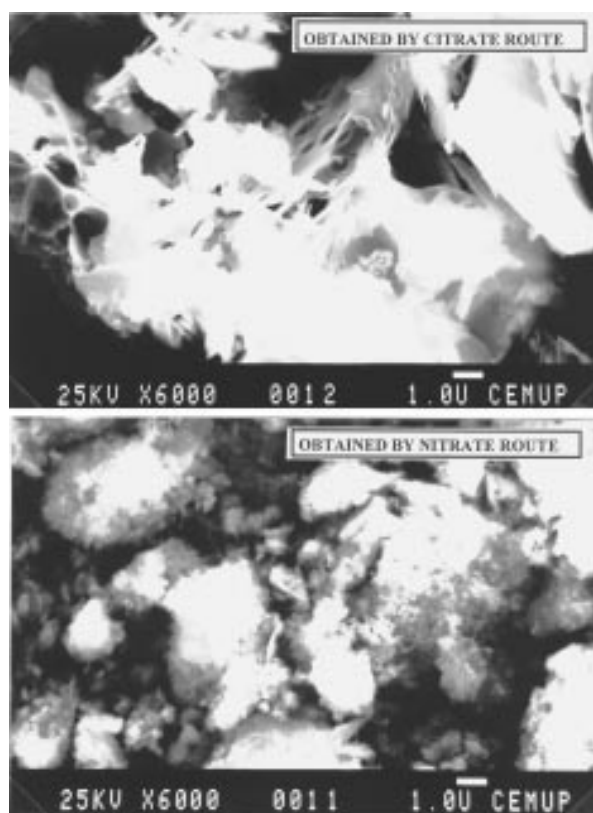


Fig. 2 SEM images of the precursor of $\text{La}_4\text{Ni}_3\text{O}_{10-8}$



Fig. 1 SEM images of the precursor of $\text{La}_3\text{Ni}_2\text{O}_{7-8}$

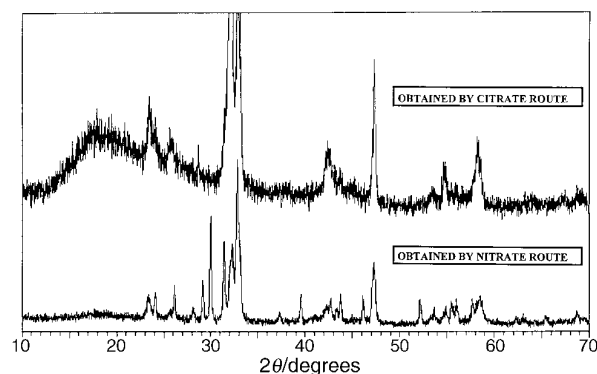


Fig. 3 X-Ray powder diffraction patterns of the precursor of $\text{La}_3\text{Ni}_2\text{O}_{7-8}$ after heating for 2 h at 1173 K

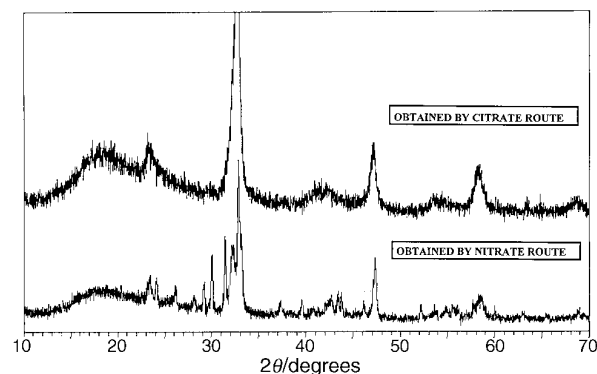


Fig. 4 X-Ray powder diffraction patterns of the precursor of $\text{La}_4\text{Ni}_3\text{O}_{10-8}$ after heating for 2 h at 1173 K

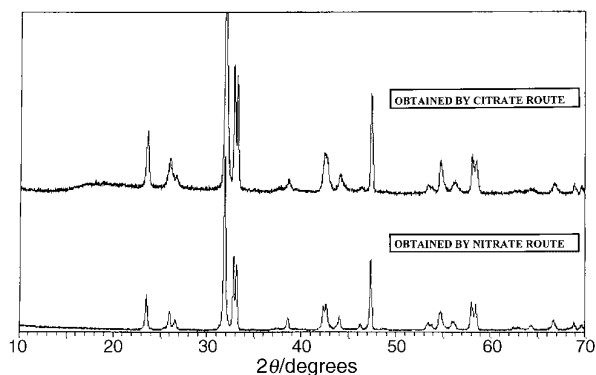


Fig. 5 X-Ray powder diffraction patterns of the final material $\text{La}_3\text{Ni}_2\text{O}_{7-\delta}$

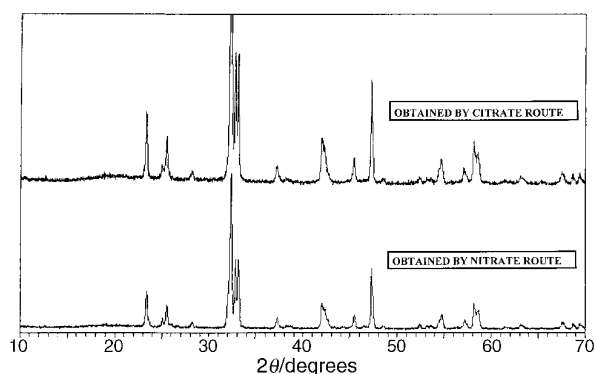


Fig. 6 X-Ray powder diffraction patterns of the final material $\text{La}_4\text{Ni}_3\text{O}_{10-\delta}$

the reaction times differing (Table 1). The compounds are pure and well crystallized. The observed XRD data were used for least-squares refinement of the unit-cell parameters in the $Fmmm$ space group. The refined unit-cell parameters are given in Table 1; they are in good agreement with those previously reported for the $n=2$ phase^{3,5,6,11} and also for the $n=3$ member.^{3,8,12,13}

However, a careful examination using high-resolution electron microscopy revealed a more complex situation. For $n=2$, one can still observe some disordered intergrowths even in the samples obtained by the citrate route. Fig. 7 shows stacking defects, which is confirmed by streaking observed in the electron diffraction pattern. For $n=3$, the citrate route leads to a well ordered structure (Fig. 8); only a few defects were observed, which was not the case for the sample prepared by the nitrate route, which showed a disordered intergrowth. Electron microscopy seems to reveal that these phases do not crystallize in the $Fmmm$ space group.

3 Chemical analysis

Quantitative chemical analyses of lanthanum and of nickel indicate a La/Ni ratio very close to 1.5 and 1.3 for $\text{La}_3\text{Ni}_2\text{O}_{7-\delta}$

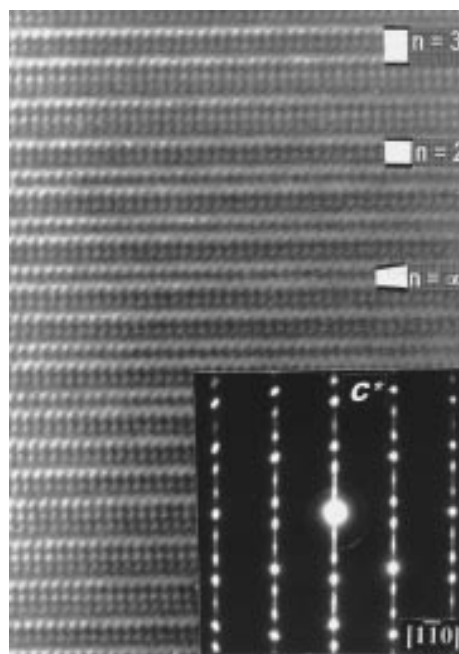


Fig. 7 High resolution electron microscopy image of $\text{La}_3\text{Ni}_2\text{O}_{7-\delta}$ (citrate route) ($[110]$ zone axis)

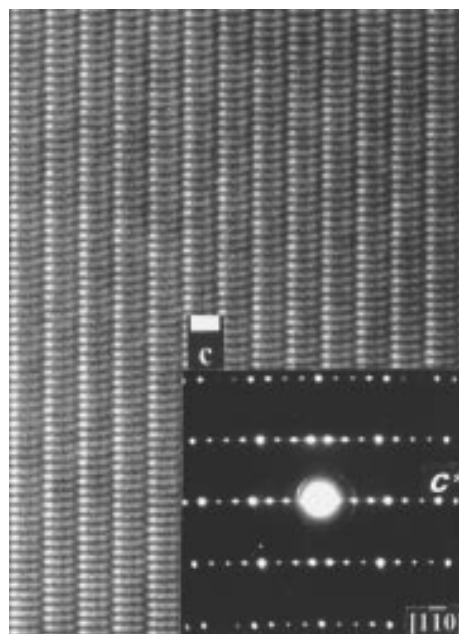


Fig. 8 High resolution electron microscopy image of $\text{La}_4\text{Ni}_3\text{O}_{10-\delta}$ (citrate route) ($[110]$ zone axis)

Table 1 Cell parameters and non-stoichiometry content of the prepared compounds

	route	reaction time/h	a^a/nm	b^a/nm	c^b/nm	V^c/nm^3	δ^d [[$(n-1-\tau)/2$]]	τ (% Ni^{3+})	formulation
$\text{La}_3\text{Ni}_2\text{O}_{7-\delta}$	nitrate	72	0.5393	0.5451	2.054	0.604	+0.07	43	$\text{La}_3\text{Ni}_2\text{O}_{6.93}$
	citrate	48	0.5400	0.5452	2.052	0.604	-0.03	53	$\text{La}_3\text{Ni}_2\text{O}_{7.03}$
$\text{La}_4\text{Ni}_3\text{O}_{10-\delta}$	nitrate	336	0.5413	0.5468	2.795	0.827	+0.25	50	$\text{La}_4\text{Ni}_3\text{O}_{9.75}$
	citrate	28	0.5415	0.5467	2.797	0.828	-0.02	68	$\text{La}_4\text{Ni}_3\text{O}_{10.02}$

^a ± 0.0002 nm. ^b ± 0.001 nm. ^c ± 0.001 nm³. ^d ± 0.02

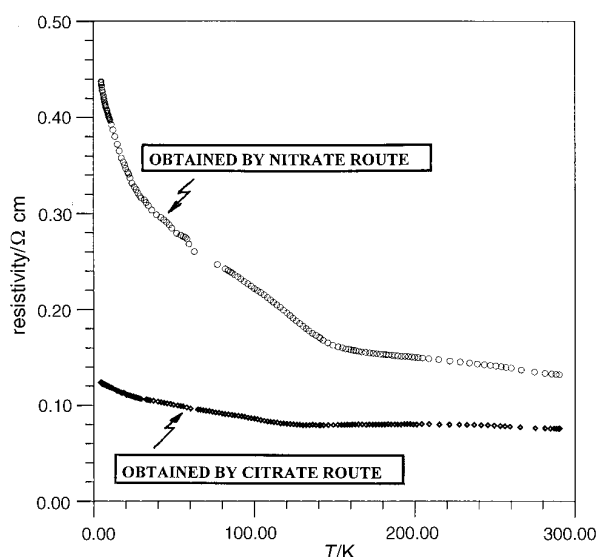


Fig. 9 Temperature dependence of the electrical resistivity for $\text{La}_3\text{Ni}_2\text{O}_{7-\delta}$

and $\text{La}_4\text{Ni}_3\text{O}_{10-\delta}$, respectively; these results are confirmed by SEM/EDS analysis.

Values of δ are reported in Table 1. For the citrate route stoichiometric compounds ($\delta=0$) were obtained, while the nitrate route samples are oxygen deficient ($\delta>0$). This result is still not very well understood since the nitrate route should be more oxidative than the citrate one. This confirms the strong influence of the morphology of the precursors on the preparation of these phases. However, it seems that the occurrence of some oxygen non-stoichiometry, δ , does not affect the cell parameters, which is in accordance with the results of Zhang *et al.*⁶

Occasionally, it has been shown that some samples prepared via the citrate route showed a small excess of oxygen, which corresponds to an oxygen over-stoichiometry likely resulting from the occurrence of interstitial oxygen atoms in the La_2O_2 layers, as was previously described for $\text{La}_2\text{NiO}_{4+\delta}$.^{14,15}

4 Electrical resistivity

Fig. 9 and 10 show the thermal dependence of the electrical resistivity, $\rho(T)$, for the $\text{La}_3\text{Ni}_2\text{O}_{7-\delta}$ and $\text{La}_4\text{Ni}_3\text{O}_{10-\delta}$ samples, respectively.

For both phases, resistivity values are always higher for the nitrate route samples than for the citrate ones. Thus, it seems that resistivity decreases with increased Ni^{3+} content, in agreement with previous work.^{3,6,11}

$\text{La}_3\text{Ni}_2\text{O}_{7-\delta}$ (Fig. 9) clearly shows a different electrical behavior depending on the preparation method, which results from the different oxygen stoichiometry of the compounds and the value of the carrier concentration is directly correlated to the $\text{Ni}^{3+}/\text{Ni}^{2+}$ ratio. Above 120 K, the metallic behavior of the citrate material agrees well with the electrical resistivity data published earlier by Moham-Ram *et al.*³ and by Zhang *et al.*⁶ for samples with similar composition. However, there is some discrepancy between these results and those of Sreedhar *et al.*⁴ who found a non-metallic behavior for this phase, but no data were given about the oxygen content of their sample. These results clearly show that the electrical resistivity is strongly dependent on δ as previously reported by Taniguchi *et al.*¹¹ However, our results are somewhat different with respect to those of these authors. In this work, a marked inflexion is visible for both samples ($\delta=0.0$ and 0.1). These inflexions occur at different temperatures: 120 K for the sample obtained by the citrate preparation and 140 K for the nitrate

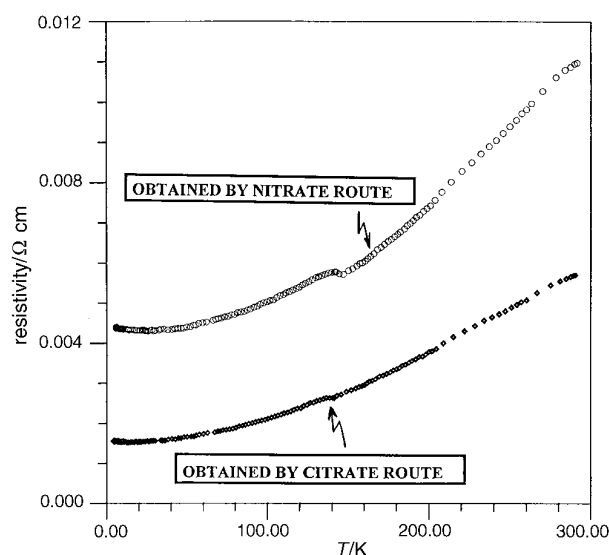


Fig. 10 Temperature dependence of the electrical resistivity for $\text{La}_4\text{Ni}_3\text{O}_{10-\delta}$

preparation. From our XRD study, no structural change was evidenced at low temperature ($77 < T \leq 298$ K). We suggest that the nature of this transition is electronic. Thus, according to Taniguchi *et al.*,¹¹ the properties of these compounds can be interpreted by a model of charge ordering in the NiO_2 planes induced by oxygen vacancy ordering, although it does not explain the observed anomaly.

For $\text{La}_4\text{Ni}_3\text{O}_{10-\delta}$, metallic behavior is always observed with a small variation in the resistivity values. These resistivity values are one order of magnitude smaller for $n=3$ compared to those for $n=2$. Moreover, the inflexion point seen at ca. 140 K in the $n=3$ sample (Fig. 10) is quite different from the metal-insulator transition seen at ca. 120–140 K in the $n=2$ sample (Fig. 9). One should point out that all the previous data for this compound present some controversy. The most recent work of Zhang *et al.*⁸ do not reveal any resistivity anomaly but Shreedhar *et al.*⁴ report an inflexion point in the curve at 140 K, but with thermal behavior differing from ours, while Tkalič *et al.*¹³ report a very marked anomaly in their work.

Additional investigations are necessary in order to give an interpretation of the observed anomalies.

Conclusion

The $n=2$ and $n=3$ members of the series $\text{La}_{n+1}\text{Ni}_n\text{O}_{3n+1-\delta}$, have been successfully synthesized using, for the first time, the citrate method. This process leads to powders which exhibit small particle sizes, which is responsible for the high reactivity of the precursors.

This work clearly shows that the preparation method has a strong influence on the oxygen stoichiometry of these compounds. It is very important to carefully measure the Ni^{3+} content, and consequently, the total oxygen content in each sample.

The samples obtained by this new method are always more oxidized than those prepared by other methods and have a higher Ni^{3+} content.

These observations are very important since they lead to variations in the physico-chemical properties of the different samples as has been shown by electrical resistivity behavior. These studies will be discussed in future work.

The authors are grateful to 'Embaixada de França em Portugal' and 'JNICT' (Portugal) for financial support.

References

- 1 P. Lacorre, *J. Solid State Chem.*, 1992, **97**, 495.
- 2 P. Lacorre, *Actual. Chim.*, 1995, **3**, 16.
- 3 R. A. Mohan-Ram, L. Ganapathi, P. Ganguly and C. R. N. Rao, *Solid State Commun.*, 1986, **63**, 139.
- 4 K. Sreedhar, M. Mc Elfresh, D. Perry, D. Kim, P. Metcalf and M. Honig, *J. Solid State Chem.*, 1994, **110**, 208.
- 5 J. Drennan, C. P. Tavares and B. C. H. Steele, *Mater. Res. Bull.*, 1982, **17**, 621.
- 6 Z. Zhang, M. Greenblatt and J. B. Goodenough, *J. Solid State Chem.*, 1994, **108**, 402.
- 7 Z. Zhang and M. Greenblatt, *J. Solid State Chem.*, 1994, **111**, 141.
- 8 Z. Zhang and M. Greenblatt, *J. Solid State Chem.*, 1995, **117**, 236.
- 9 P. Dordor, E. Marquestaut and G. Villeneuve, *Rev. Phys. Appl.*, 1985, **20**, 795.
- 10 P. Barboux, P. Griesmar, F. Ribot and L. Mazerolles, *J. Solid State Chem.*, 1995, **117**, 343.
- 11 S. Taniguchi, T. Nishikawa, Y. Yasui, Y. Kobayashi, J. Takeda, S. I. Shamoto and M. Sato, *Phys. Soc. Jpn.*, 1995, **64**, 1644.
- 12 C. Brisi, M. Vallino and F. Abbattista, *J. Less Common Met.*, 1981, **79**, 215.
- 13 K. Tkalic, V. P. Glazkov, V. A. Somenkov, S. Shil'Shteoin, A. E. Kar'Kin and A. V. Mirmel'Shtein, *Superconductivity*, 1991, **4**, 2280.
- 14 A. Demourgues, F. Weill, J. C. Grenier, A. Wattiaux and M. Pouchard, *Physica C*, 1992, **192**, 425.
- 15 A. Demourgues, F. Weill, B. Darriet, A. Wattiaux, J. C. Grenier, P. Gravereau and M. Pouchard, *J. Solid State Chem.*, 1993, **106**, 317.

Paper 7/02424J; Received 9th April, 1997